

Novel Non-Contact Optical Fiber Displacement Sensor Using Bidirectional Modulation of a Mach-Zehnder Electro-Optical Modulator

Hyeon-Ho Kim¹, Sang-Jin Choi¹, Hao Yi¹, Keum Soo Jeon², and Jae-Kyung Pan¹

¹Dept. of EE and Smart Grid Research Center, Chonbuk National University, Jeonju, Republic of Korea

²Wind Valley Co. Ltd., Suncheon, Republic of Korea

Paper Summary

A novel non-contact optical fiber displacement sensor is proposed and analyzed. The linear relationship between the time delay and displacement variation is given, which is based on a bidirectional modulation of a Mach-Zehnder electro-optical modulator.

Introduction

The problem of measuring short distances without contact arises in several areas of engineering and particularly in precision micro-mechanics for monitoring small moving parts. Non-contacting measuring has two chief methods based on optical principle and electromagnetic principle. Historically, free space optics has been used in these cases, exploiting for example interferometry or triangulations [1]; however, in an industrial context, a fiber based sensor provides further interesting features, such as an intrinsic simplification in positioning the sensing optical beam in front of the moving object, joined with impossibility to start fires and complete electromagnetic immunity, due to the possibility to place the electronic control circuitry in a remote safe and electromagnetic quiet environment.

A brief overview of the measurement of linear displacement by optical or electro-optical means was presented [1]. A non-contact and low-cost distance sensor aimed at applications where displacements up to few millimeters in micromechanics was reported [2]. C. Prella et al. presented a miniature optical displacement sensor with millimetric range and nanometric resolution and a fiber optic sensor for two-dimensional linear displacement measurements [3,4]. A non-contacting magnetic coupling displacement sensor based on fiber Bragg grating (FBG) sensing technology was researched, which combines advantages of FBG sensor with ones of magnetic measuring methods such as flame protection, remote monitoring, oil corrupt, work in dust-laden atmosphere [5]. A bidirectional modulation of a Mach-Zehnder electro-optical modulator (MZ-EOM) has been used to measure the optical fiber chromatic dispersion [6] and to implement a RF interrogation structure of a fiber Bragg grating sensor [7].

In this paper, we propose and analyze a novel non-contact optical fiber displacement sensor based on bidirectional modulation of an MZ-EOM. The relationship between the time delay and displacement variation is given.

Theory and experimental setup

The proposed non-contact optical fiber displacement sensor, which consists mainly of a tunable laser, MZ-EOM, optical collimator, specular object, and photodetector (PD), is shown in Fig. 1. Light from the tunable laser passes through port 1 of a three-port circulator and goes into the polarization controller in port 2. After passing through the polarization controller, the light is modulated by an RF signal via the MZ-EOM with co-propagation, i.e., propagation in the same direction as the light (as indicated by the arrow in the diagram of the MZ-EOM shown in Fig. 1). The unidirectional modulated light is reflected by the specular object, i.e., mirror and is modulated by an RF signal via the MZ-EOM with counter-propagation, i.e., propagation in the opposite direction to the light. The bidirectional modulated light is received by the PD and measured by the network analyzer (NA). The modulating process in Fig. 1 can be considered as an equivalent model, shown in Fig. 2, with two MZ-EOMs cascaded in series [6].

The travel time in terms of the displacement of the proposed optical fiber displacement sensor, $\tau(d)$, can be expressed as:

$$\tau(d) = \tau_{fiber} + \tau_{free}(d) = \frac{2L_{fiber}}{v_g} + \frac{2(D_o + d)}{c} \quad (1)$$

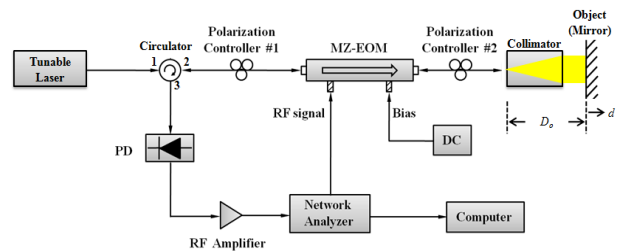


Fig. 1. Experimental setup for the proposed non-contact optical fiber displacement sensor. MZ-EOM: Mach-Zehnder electro-optical modulator. PD: photodetector.

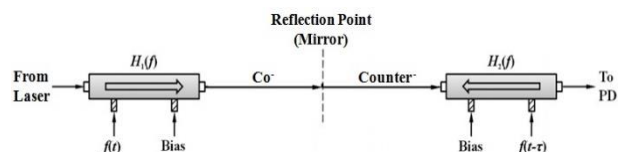


Fig. 2. Equivalent model of bidirectional modulation with an MZ-EOM and a mirror.

where τ_{fiber} is the travel time spent in the optical fiber between the MZ-EOM and collimator, $\tau_{free}(d)$ is the travel time spent in free space between the end of optical fiber and object, L_{fiber} is the length of the optical fiber between the MZ-EOM and collimator, v_g is the group velocity of light in the optical fiber, D_o is the length of free space between the end of optical fiber and object, d is the displacement from the original point, c is the light velocity in free space.

The time delay, $\Delta\tau(d)$, which is the difference in the travel time for the original point and the displacement, d , can be expressed as:

$$\Delta\tau(d) = \tau(d) - \tau(0) = \frac{2d}{c} \quad (2)$$

From Eq. (2), we can see that the time delay and the displacement have a linear relationship.

In the course of propagation, the first MZ-EOM in Fig. 2 causes the forward propagating light in Fig. 1 to experience co-propagating modulation by the RF signal $f(t)$. On the other hand, the second MZ-EOM in Fig. 2 causes the back-reflected light in Fig. 1 to experience counter-propagating modulation caused by the RF signal $f(t - \tau)$. Assuming that the modulation indices are very small and the biasing is set at the quadrature point, we can obtain an expression for the output optical power $P_{out}(t)$ at the PD as [6]:

$$P_{out}(t) = \frac{P_{in} T_D}{4} [1 + m_1 H_1(f) \cos 2\pi f t] \cdot [1 + m_2 H_2(f) \cos 2\pi f (t - \tau)] \quad (3)$$

where P_{in} is the input optical power, T_D indicates the coupling and optical transmission losses of the structure, m_1 and m_2 are the modulation indices of co-propagating and counter-propagating modulation, respectively, and $H_1(f)$ and $H_2(f)$ are the transfer functions for co-propagating and counter-propagating modulation of the MZ-EOM, respectively.

The DC and harmonic components in Eq. (3) are eliminated at the PD and the NA because all vector NAs use a tuned-receiver (narrow-band) architecture to reject harmonic and spurious signals. Consequently, if it is assumed that $m_1 = m_2 = m$, the total transfer function $H(f)$ measured at the NA can be written as:

$$H(f) = A_0 [H_1(f) + e^{-j2\pi f \tau} H_2(f)] \quad (4)$$

where $A_0 = m R G_m P_{in} T_D / 4$, R is the responsivity of the PD, and G_m is the gain of the RF amplifier. The free spectral range (FSR) is formed by ripples in the transfer function and depends on the travel time in Eq. (4), which is in turn strongly related to the period of the ripples. The FSR according to the displacement can be expressed as:

$$FSR_d = \frac{1}{\tau(d)} \quad (5)$$

Upon measuring the change in the FSR based on the displacement variation, the travel time and time delay can be calculated from Eqs (1, 2, 5).

Measurement and results

Fig. 3 shows the simulation results obtained with the proposed optical fiber displacement sensor, namely the transfer function $H(f)$ for seven different displacements over the modulation frequency range from 250 MHz to 450 MHz, assuming L_{fiber} of 1.5 m, D_o of 84 mm, and the refractive index of the optical fiber of 1.4681. Obviously, as the displacement increases, the corresponding FSR reduces. It is very helpful to

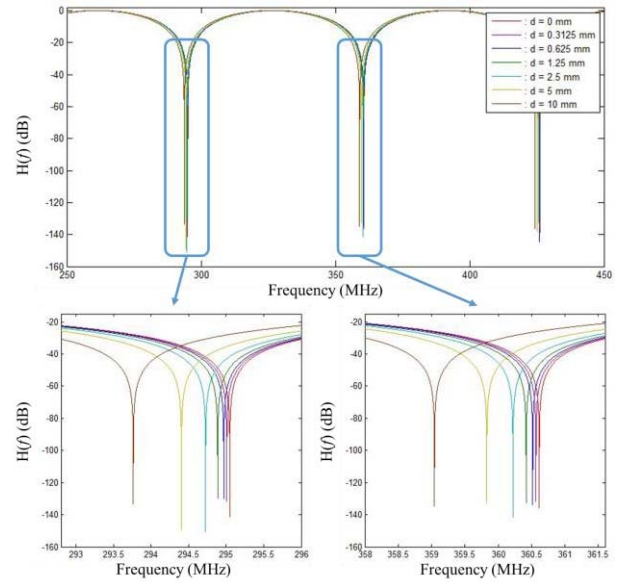


Fig. 3. Calculated transfer function $H(f)$ for seven displacements with L_{fiber} of 1.5 m, D_o of 84 mm, and the refractive index of the optical fiber of 1.4681 in the frequency range of 250 MHz to 450 MHz.

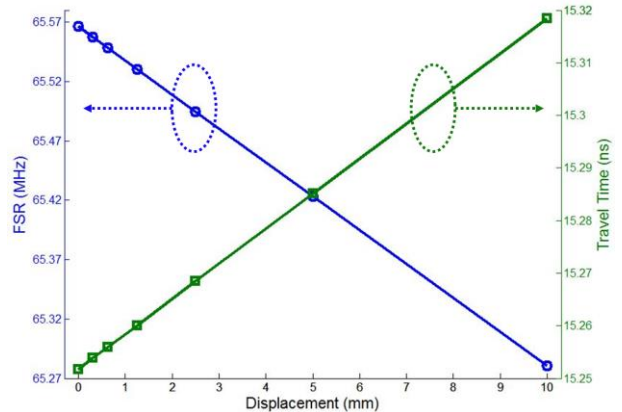


Fig. 4. The FSR (blue line) and the travel time (green line) according to the displacement variation of the proposed optical fiber displacement sensor.

distinguish the displacement variation if the optical fiber length, L_{fiber} , can be as short as possible. Furthermore, the characteristic of two transfer functions $H_1(f)$ and $H_2(f)$ are utterly unlike except that the modulation frequency range is significantly lower than the bandwidth of the MZ-EOM, then the optimal measuring range should be selected near the frequency of 500 MHz.

From Fig. 3, the FSRs can be determined for seven displacements, which are shown in Fig. 4. Fig. 4 also shows travel times corresponding to the FSRs for seven displacements, which are 15.252 ns and 15.318 ns at the first displacement of 0 mm and the last displacement of 10 mm, respectively. We confirmed that the relationship between the time delay and the displacement variation is linear with a gradient of 6.6 ps/mm. The system performance, such as the maximum measurement range and the resolution, can be further improved by using a shorter optical fiber length between MZ-EOM and mirror, an increased number of NA sampling points, and an optical source with larger output power.

Conclusions

We have proposed and analyzed a non-contact optical fiber displacement sensor using bidirectional modulation of an MZ-EOM. The travel time variation according to the displacement variation has been calculated from the transfer function of a bidirectional modulation of an MZ-EOM. As the displacement changes from 0 to 10 mm, the FSR and travel time change from 65.5662 to 65.2807 MHz and from 15.252 to 15.318 ns, respectively. In this study, a good linear relationship between the time delay and displacement variation with a gradient of 6.6 ps/mm has been achieved. We now focus on the implementation of the proposed sensor model.

Acknowledgments

This work was supported by a National Research Foundation of Korea (NRF) grant funded by the Korean government (MEST) (2010-0028509) and by the Basic Science Research Program through the NRF funded by the MEST (2011-0010473).

References

1. P. M. B. S. Girão et al., IEEE Sens. J. vol. 1, no. 4 (2001) pp. 322-331
2. M. L. Casalicchio et al., I2MTC 2009 (2009) pp. 1671-1675
3. C. Prelle et al., Sensors and Actuators A 127 (2006) pp. 139-146
4. A. Khiat et al., Sensors and Actuators A 158 (2010) pp. 43-50
5. H. K. MI et al., Proc. the 2011 IEEE International Conference on Mechatronics and Automation (2011) pp. 2443-2447
6. K. S. Jeon et al., IEEE Photon. Tech. Lett. 14 (2002), pp. 1145-1147
7. S. J. Choi et al., Sensors 13 (2013) pp. 8403-8411